Direct Data-Driven Vibration Control for Adaptive Optics

Vaibhav Gupta[1], Alireza Karimi[1], François Wildi[2] and Jean-Pierre Véran[3]

***Abstract*— Adaptive optics (AO) systems are used in ground-based telescopes to improve image resolutions, especially for long-exposure photography, by compensating for the effects of atmospheric turbulence and internal vibrations. Most current AO systems are based on simple control laws that either neglect the temporal correlation in atmospheric turbulence, use a simplified system model, or both. This paper presents a direct data-driven control scheme to compute an optimal controller using the frequency-domain representation of the disturbance and the system model. Numerical simulations of the AO system demonstrate performance improvement compared to standard AO control schemes, and resilience to the variance in atmospheric turbulence and internal vibrations.**

I. Introduction

Adaptive optics (AO) is used to improve the image quality captured by ground-based telescopes and other optical instruments by actively sensing, estimating, and correcting the wavefront distortions as the light passes through a turbulent medium like Earth's atmosphere. AO has improved ground-based astronomical imaging bringing it closer to the diffraction limit of the light [1], [2]. However, to achieve extremely long-exposure photography and improve imaging performance, compensation for the vibration of the telescope structure, in addition to wavefront distortion caused by the atmosphere, is needed. In European Southern Observatory (ESO) 3.6 m telescope, it has been noted that the vibrations of the telescope due to the wind and other observatory components such as cryocoolers, motors and fans can reduce the performance by 10 % in the H-band (infrared with a wavelength of 1.65 µm) [3]. A more performant controller for tip/tilt, which is primarily affected by mechanical vibrations, can lead to significant enhancements in the imaging performance of AO systems.

Most current AO systems use a modal controller modelled as a leaky integrator controller, which is tuned to have the best compromise between the atmospheric disturbance rejection and measurement noise amplification [4], [5]. However, this approach does not take advantage of the correlation in the disturbance due to atmospheric turbulence in short to medium timescales. To address this, AO systems with predictive control methods are an active area of interest. Some methods which use the statistical models of atmospheric turbulence, with some assumptions on its structure, have been proposed [6], [7]. Controllers designed by first estimating the dynamics of the disturbance either online using recursive optimisation [8], or using subspace identification [9] have been proposed. Still, the selection of the order of the disturbance representation is a tricky and ongoing part of the effort. On the other end of the spectrum, methods for forecasting wavefront errors [10], [11] and using the forecast for feed-forward compensation have seen success in error reduction during on-sky operations [12]. The compensation is computed by assuming a simplified temporal model of the AO system, represented as some multiple frame delays, which can introduce significant conservatism, especially when the guide star is dim and a slow control loop is required. In [13], the frequency spectrum of the disturbance is used for designing and optimising the controller, but this approach requires a parametric model of the AO system.

Since the desired performance can be represented in the frequency domain, data-driven methods using only frequency-domain data to compute an optimal controller are studied. The controller design using frequency-domain data leads to a non-convex optimisation problem but several convex approximations have been proposed in the literature. [14] and [15] utilises the frequency-domain data for the computation of SISO-PID controller by convex optimisation, employing the constraint linearisation similar to [16]. MIMO-PID controller synthesis is presented as a convex-concave optimisation in [17] and solved by linearisation of quadratic matrix inequalities. [18] adopts similar linearisation to compute linearly parameterised controllers. A frequency-based data-driven control design methodology is proposed in [19], featuring an $\mathcal{H}_\infty$ control objective, based on coprime factorisation of the controller. Finally, a fixed-structure data-driven controller design method with mixed $\mathcal{H}_2/\mathcal{H}_\infty$ sensitivity performance is proposed in [20].

The contribution of this paper is to present an innovative control strategy for AO systems that utilises input-output data of the system and the disturbance spectrum due to atmospheric turbulence. In contrast to the approach outlined in [13], the proposed method does not require a parametric model of the AO system; only its frequency response is needed. The approach eliminates the need for a disturbance model and can even account for the fractional time delay in the AO system. Additionally, the resulting controller displays remarkable robustness to atmospheric changes and external disturbances, resulting in nearly optimal control performance for short to medium-term variations.

The paper is structured as follows: In Section II, a description of a generic AO system and the problem statement are provided. The proposed control schema is presented in Section III, and in Section IV, various numerical simulations

[1]V. Gupta and A. Karimi are with Laboratoire d'Automatique, École Polytechnique Fédérale de Lausanne, CH-1015 Lausanne, Switzerland vaibhav.gupta@epfl.ch

[2]F. Wildi is with Départment d'astronomie, Université de Genève, 51 ch. des Maillettes Sauverny, CH-1290 Versoix, Switzerland

[3]J.-P. Véran is with National Research Council, Herzberg Institute of Astrophysics, 5071 W. Saanich Rd, Victoria, BC, V9E 2E7, Canada

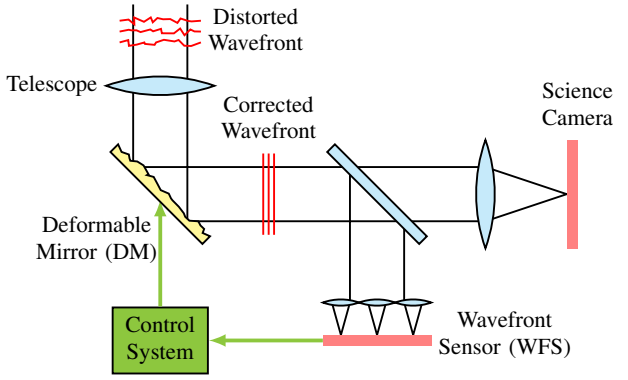

Fig. 1: Typical AO system

are presented for the Near-IR Adaptive Optics System (NFIRAOS) [21] of the Thirty Meter Telescope (TMT) [22]. In Section V, we discuss potential outlooks for implementing the control scheme, accompanied by concluding remarks.

II. Adaptive Optics (AO) System

In Fig. 1, a typical AO system is presented. The light travelling from the stars to the Earth is expected to have a flat wavefront, but as it passes through the turbulent atmosphere of the Earth, it becomes distorted by the time it reaches the ground-based telescopes. To correct this distortion, the AO systems within the telescope use a deformable mirror (DM) to actively control the path lengths of the light. The incoming light with a distorted profile $\varphi(\cdot)$ is directed to DM, which applies a phase correction $\varphi^{corr}(\cdot)$. The reflected beam with a residual profile $\varphi^{res}(\cdot)$ is split into two components: one to a wavefront sensor (WFS) and the other to the science camera for imaging. The WFS provides a quantitative measure of the residual wavefront distortion denoted by $\vec{p}$, which is used to compute the DM actuator commands $\vec{v}$.

Typically, the wavefront is decomposed into different modes, using some orthogonal basis, such that they can be controlled individually. The translation matrices that link the modes to the wavefront sensor (WFS) output M and the deformable mirror (DM) inputs D are computed allowing all the modes to be treated as parallel single-input single-output (SISO) control problems. Fig. 2 illustrates the complete control system for the typical AO system with the computational delay due to wavefront computer (WFC). Fig. 3 illustrates the SISO control loop for a single mode, where disturbance $d(t)$ and error $e(t)$ represent the modal components of $\varphi(\cdot)$ and $\varphi^{res}(\cdot)$ respectively. For more insight into the field of AO systems and their modal control, readers are directed to [23], [5], [24], [25].

A common measure of the overall performance of an AO system is the Strehl ratio, defined as the on-axis intensity of a point source relative to the diffraction limit intensity. Using Maréchal's approximation [26], it can be shown that the maximisation of the Strehl ratio is equivalent to the minimisation of the mean-squared error of the phase. With an appropriate choice of modal decomposition method, the sum of the mean-squared errors of each mode can provide a good approximation of the mean-squared error of the phase over the aperture. Hence, the control objective is to minimise the 2-norm of the error for each parallel SISO problem.

The problem considered in this paper is designing the optimal fixed-structure controller for each mode, given open-loop WFS observations of the disturbance and the photon flux of the guide star. Furthermore, the non-parametric system is considered, enabling the inclusion of more complex system dynamics. Large telescopes can have AO control loops operating at frequencies in the order of 1 kHz, with the total number of controlled modes potentially reaching up to 1000. Therefore, the digital IIR filter has been consideration as the fixed-structure controller because of its relatively low computational and implementation complexity.

III. Data-driven Control Schema

The proposed control scheme differs from the current state-of-the-art schemes in that it does not rely on an assumed or identified model of the disturbance. Instead, the scheme utilises a sample of the disturbance to estimate its frequency response [27], which is subsequently used in the design of the controller. First, the control objective is converted from the minimisation of the 2-norm of the time-domain error to an equivalent objective in the frequency-domain. Then, the objective is transformed into an iterative convex optimisation problem for optimal fixed-structure controller synthesis.

Notations

$M \succ (\succeq) N$ indicates that $M-N$ is a positive (semi-) definite matrix and $M \prec (\preceq) N$ indicates $M-N$ is negative (semi-) definite. The transpose of a matrix M is denoted by M^T and its conjugate transpose by M^*.

A. Control objective

The objective of the desired controller $K(z)$ is to minimise the 2-norm of the error signal $\|e\|_2$. The spectrum of $e(t)$, $E(e^{j\omega})$, can be represented as

$$E(e^{j\omega}) = \mathcal{D}(e^{j\omega})D(e^{j\omega}) - \mathcal{N}(e^{j\omega})N(e^{j\omega}) \tag{1}$$

where, $D(e^{j\omega})$ and $N(e^{j\omega})$ are the spectra of $d(t)$ and $n(t)$ respectively,

$$\mathcal{D}(e^{j\omega}) = \frac{1}{1+K(e^{j\omega})\ \mathrm{DM}(e^{j\omega})\ \mathrm{WFC}(e^{j\omega})\ \mathrm{WFS}(e^{j\omega})},$$
$$\mathcal{N}(e^{j\omega}) = \frac{K(e^{j\omega})\ \mathrm{DM}(e^{j\omega})\ \mathrm{WFC}(e^{j\omega})}{1+K(e^{j\omega})\ \mathrm{DM}(e^{j\omega})\ \mathrm{WFC}(e^{j\omega})\ \mathrm{WFS}(e^{j\omega})},$$

and $K(e^{j\omega})$, $\mathrm{DM}(e^{j\omega})$, $\mathrm{WFC}(e^{j\omega})$, and $\mathrm{WFS}(e^{j\omega})$ are the frequency responses of $K(z)$, DM, WFC, and WFS respectively. The flux noise can be assumed to be white noise with variance ς which is dependent on the flux of the guide star and the readout noise of the wave-front sensor. Hence, the expectation of the squared 2-norm of the error signal is

$$\mathbb{E}\left(\|E\|_2^2\right) = \|D\mathcal{D}\|_2^2 + \|\varsigma\mathcal{N}\|_2^2. \tag{2}$$

Then the control objective can be chosen as,

$$\min\left(\|W_d\mathcal{D}\|_2^2 + \|W_n\mathcal{N}\|_2^2\right) \tag{3}$$

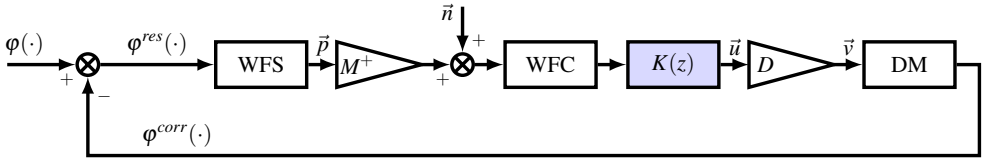

Fig. 2: Complete control loop for a typical AO system

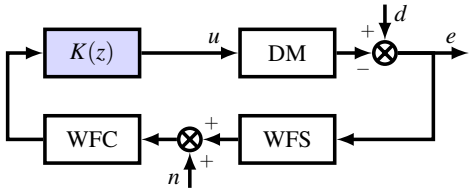

Fig. 3: Control loop for a single mode of a typical AO system

where $W_d(e^{j\omega}) = D(e^{j\omega})$ and $W_n(e^{j\omega}) = \alpha\varsigma$ are the filters for disturbance rejection and noise minimisation respectively. The parameter α serves as the trade-off factor that governs the balance between disturbance rejection and noise minimisation. This parameter can be finely tuned to align with the hardware specifications and robustness requirements.

B. Data-driven controller optimisation

The direct data-driven frequency-domain controller synthesis for (3) can be written as the optimisation [20],

$$\min_{K(z),\Gamma(\omega)} \frac{1}{2\pi}\int_{\Omega}\Gamma(\omega)\,\mathrm{d}\omega \tag{4}$$

$$s.t. \quad \text{Closed loop is internally stable}$$
$$(W_d\mathcal{D})(W_d\mathcal{D})^* + (W_n\mathcal{N})(W_n\mathcal{N})^* \preceq \Gamma \qquad \forall\omega\in\Omega$$

where $\Gamma(\omega)$ is a frequency dependent scalar and Ω is the stability boundary for discrete-time systems,

$$\Omega = \left\{ z\in\mathbb{C} \;\middle|\; z = e^{j\omega},\ \omega\in[0,2\pi) \right\}.$$

Since the controller is assumed to be a digital IIR filter, it can be factorised as $K(z) = X(z)Y^{-1}(z)$ with

$$X(z) = \sum_{k=0}^{n} X_k z^{-k} \quad \text{and} \quad Y(z) = \sum_{k=0}^{n} Y_k z^{-k}$$

where, X_k and Y_k are the optimisation variables. Then the constraint in (4) can be written as,

$$\begin{bmatrix} W_dY & \bar{W}_nX \end{bmatrix} \begin{bmatrix} \Phi^*\Phi & 0 \\ 0 & \Phi^*\Phi \end{bmatrix}^{-1} \begin{bmatrix} (W_dY)^* \\ (\bar{W}_nX)^* \end{bmatrix} \preceq \Gamma$$

where,

$$\begin{aligned} \bar{W}_n(e^{j\omega}) &= W_n(e^{j\omega})\ \mathrm{DM}(e^{j\omega})\ \mathrm{WFC}(e^{j\omega}),\\ \Phi(e^{j\omega}) &= Y(e^{j\omega}) + G(e^{j\omega})\ X(e^{j\omega}),\\ G(e^{j\omega}) &= \mathrm{DM}(e^{j\omega})\ \mathrm{WFC}(e^{j\omega})\ \mathrm{WFS}(e^{j\omega}). \end{aligned}$$

Using the Schur complement lemma, an equivalent matrix inequality can be found,

$$\begin{bmatrix} \Gamma & \mathcal{L} \\ \mathcal{L}^* & (\Phi^*\Phi)I \end{bmatrix}(e^{j\omega}) \succeq \mathbf{0} \qquad \forall\omega\in\Omega \tag{5}$$

where, $\mathcal{L} = \begin{bmatrix} W_dY & \bar{W}_nX \end{bmatrix}$. This inequality is convexified around a known initial controller $K_c = X_cY_c^{-1}$, using a lower bound on $\Phi^*\Phi$:

$$\Phi^*\Phi \succeq \Phi^*\Phi_c + \Phi_c^*\Phi - \Phi_c^*\Phi_c$$

where, $\Phi_c = Y_c + GX_c$. This gives a convex optimisation problem with linear matrix inequalities,

$$\min_{X_k,Y_k,\Gamma(\omega)} \frac{1}{2\pi}\int_{\Omega}\Gamma(\omega)\,\mathrm{d}\omega \tag{6}$$

$$\text{s.t.} \quad \begin{bmatrix} \Gamma & \mathcal{L} \\ \mathcal{L}^* & (\Phi^*\Phi_c + \Phi_c^*\Phi - \Phi_c^*\Phi_c)I \end{bmatrix}(e^{j\omega}) \succeq \mathbf{0} \qquad \forall\omega\in\Omega$$

If the known initial controller K_c is stabilising, then using [20, Theorem 2], it can be proven that the designed controller K is also stabilising. The objective can be shown to be non-increasing, as the initial controller is always a feasible solution and the problem is convex in the optimisation parameters. So, the final controller will converge to a local minimum or a saddle point of the original problem. The optimisation problem can be solved by gridding over the frequencies and using the designed controller as the initial stabilising controller for the next optimisation. Note that the controller synthesis only needs the evaluation of the filters and system at the selected frequency points. Therefore, it is possible to directly employ the non-parametric frequency responses in the optimisation procedure.

The required non-parametric frequency responses can be estimated using the Fourier analysis method from the finite input/output sampled data. For example, the frequency response of $P(e^{j\omega})$ can be computed $\forall\omega\in[0,\pi/T_s)$ as [27]:

$$P(e^{j\omega}) = \left[\sum_{k=0}^{N-1}\mathbb{I}(k)e^{-j\omega T_s k}\right]\left[\sum_{k=0}^{N-1}\mathbb{O}(k)e^{-j\omega T_s k}\right]^{-1} \tag{7}$$

where N is the number of data points for each experiment, T_s is the sampling period, and each column of $\mathbb{I}(k)$ and $\mathbb{O}(k)$ represents respectively the inputs and the outputs at sample k from one experiment. It is assumed that the input signal is persistently exciting.

For the robust controller synthesis, an additional constraint on the modulus margin m of the closed loop system is added.

$$\|\mathcal{D}\|_\infty \le m^{-1} \implies (m\mathcal{D})(m\mathcal{D})^* \preceq 1 \qquad \forall\omega\in\Omega$$

This can be converted into linear matrix inequality and added

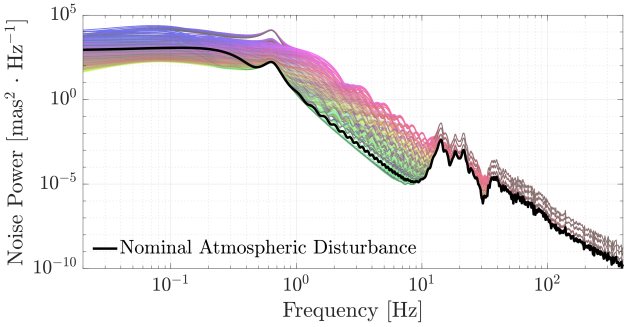

Fig. 4: Disturbance spectrum for variations in the atmospheric conditions

as an additional constraint.

$$\min_{X_k, Y_k, \Gamma(\omega)} \frac{1}{2\pi} \int_\Omega \Gamma(\omega)\, \mathrm{d}\omega \tag{8}$$

$$\text{s.t.} \quad \begin{bmatrix} \Gamma & \mathcal{L} \\ \mathcal{L}^* & (\Phi^*\Phi_c + \Phi_c^*\Phi - \Phi_c^*\Phi_c) I \end{bmatrix} (e^{j\omega}) \succeq \mathbf{0} \qquad \forall \omega \in \Omega$$

$$\begin{bmatrix} I & mY \\ (mY)^* & \Phi^*\Phi_c + \Phi_c^*\Phi - \Phi_c^*\Phi_c \end{bmatrix} (e^{j\omega}) \succeq \mathbf{0} \qquad \forall \omega \in \Omega$$

IV. Numerical Simulations

In principle, the proposed schema is agnostic to the mode in question and can be used for designing controllers for all modes of the AO system. However, in this paper, only tip/tilt modes are considered. This is because up to 90 % of the wavefront error is in the tip/tilt modes, and designing controllers for these modes can result in significant performance improvement with minimal increase in complexity. The proposed schema is compared to the classical control scheme used in the AO system, an 'integrator' controller with an optimised gain, and to a more state-of-the-art control scheme, a 'Type2' controller consisting of two cascaded integrators along with an optimal gain and a lead filter to ensure stability [28], [29].

This study simulates disturbances in the the Near-IR Adaptive Optics System (NFIRAOS) [21] of the Thirty Meter Telescope (TMT) [22] due to atmospheric turbulence, telescope windshake, and internal vibrations in the AO system. The telescopic windshake is modelled using FEM study of the telescope and the environment [30]. Transient displacement time series due to the vibration of TMT are applied to the NFIRAOS mounting locations and displacement/rotation responses for each optical element are computed to generate wavefront error variations [31]. Fig. 4 shows the variations in total disturbance observed under different observation conditions (see table I). For the NFIRAOS system, the typical sampling frequency is 100 Hz to 800 Hz. Measurement noise arises from flux noise and sensor readout. Sensor readout noise is more significant in conventional detectors. The study designs tip/tilt controllers of order 5 to minimise computational load and reduce closed-loop error signals.

The performance of the controller is measured as the attenuation of the open-loop RMS. The attenuation of the

TABLE I: Variations in the atmospheric conditions

	Variations	Nominal Condition
Wind speed [m s^{-1}]	5 to 50	10
Fried's parameter []	0.08 to 0.30	0.15
External scale of turbulence [m]	15 to 40	30
Gain for instrument disturbance []	1 to 10	1
Percentile scale of windshake for TMT [%]	50 to 95	50

RMS value in dB is given by,

$$\text{Attenuation} = 20\log_{10}\left(\frac{\text{RMS}_{CL}}{\text{RMS}_{OL}}\right) \tag{9}$$

where, RMS_{CL} and RMS_{OL} are the closed-loop and open-loop RMS of the error signal respectively.

A. Effect of variations in photon flux

A user of the AO system has access to the photon flux of the guide star a priori and needs to choose an appropriate sampling frequency for the AO system based on this information. To assist with this process, a chart correlating the photon flux to the sampling frequency is generated and provided to the user.

Fig. 5 depicts the performance of various controllers under two scenarios: one without readout noise in the WFS sensor and the other with a small amount of readout noise. In the noise-free case, higher sampling frequencies benefit integrator and Type2 controllers' attenuation at high photon fluxes, while the data-driven controller's attenuation doesn't depend on the sampling frequency. With readout noise, higher sampling frequencies improve attenuation for high photon fluxes but worsen it for low photon fluxes for all controllers. Crucially, the data-driven controller consistently outperforms the other controllers across the entire range of photon fluxes.

B. Effect of variation in atmospheric conditions

This sub-study aims to account for changing atmospheric conditions during observations, requiring robustness. The nominal sampling frequency of 400 Hz and 1600 photons per timestep is chosen representing a fairly bright guide star. Atmospheric condition variations are detailed in table I and the 'average' night at the location representing the nominal condition. The 'robust' control scheme gathers initial data and computes the controller for the entire observation duration.

Robust controllers using the three approaches are designed for the nominal atmospheric condition by setting appropriate robustness margins, and their performances are compared for different atmospheric conditions. For the integrator, manual tuning of the gain is done to achieve the desired robustness whereas, for the Type2 controller, the lead filter is tuned to obtain the desired phase margin of 45°. As for the proposed approach, an additional constraint is added to attain a modulus margin of 0.5 as described in (8).

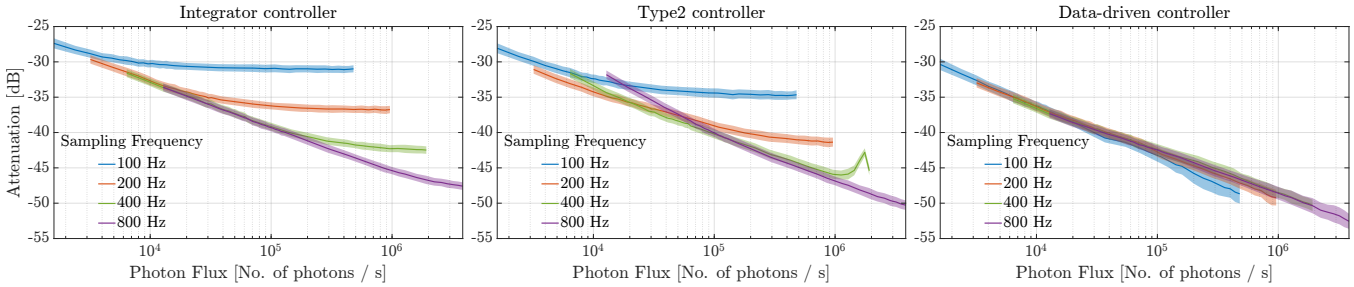

(a) WFS sensor with no readout noise

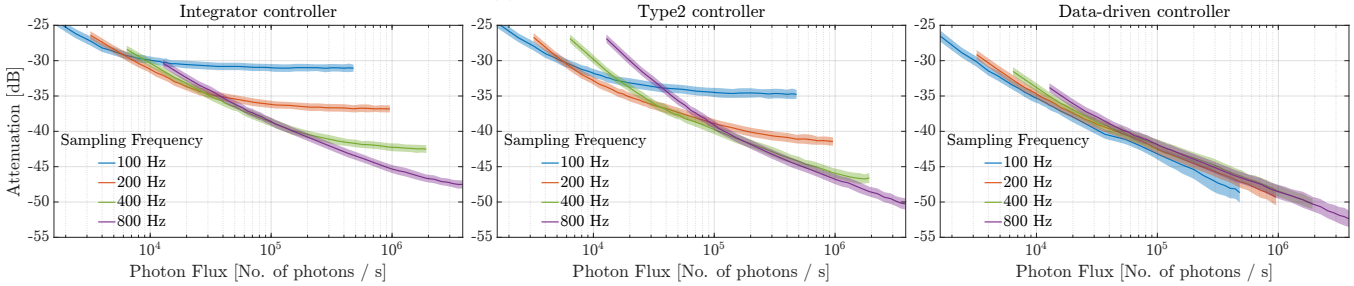

(b) WFS sensor with some readout noise

Fig. 5: Attenuation under variations in photon flux

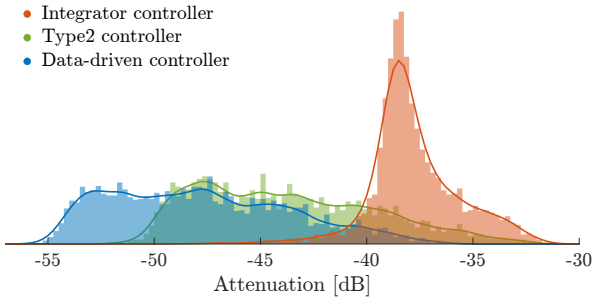

Fig. 6: Probability density function (PDF) of the achieved attenuation for the variations in the atmospheric conditions

Fig. 6 shows the probability density function (PDF) of the attenuation of the controllers. Not only does the data-driven controller outperform other controllers, but it also exhibits reduced sensitivity to variations in atmospheric conditions.

C. *Effect of external narrowband disturbance*

Some electrical components such as cryocoolers, motors and fans can introduce sinusoidal narrowband disturbances, typically 30 Hz to 60 Hz, to the AO system. Since these disturbances are usually active for a significant time, the controller should have a good rejection for these disturbances. The study assumes that only the presence of the disturbance is known, but not its actual characteristics. For integrator and Type2 controllers, the gains are re-optimised, whereas the proposed approach involves adding a peak filter, with a centre frequency of 45 Hz and bandwidth of 15 Hz, to the W_d to indicate the presence of the narrowband disturbance.

Table II gives different variations of the narrowband disturbance considered in the study. It can be observed from Fig. 7 that there is an attenuation gain of 20 dB to 25 dB against integrator, and 25 dB to 30 dB against Type2 controller.

TABLE II: Variations of the external narrowband disturbance

	Variations
RMS [mas]	1 to 21
Centre frequency [Hz]	40 to 50
Bandwidth [Hz]	6 to 30

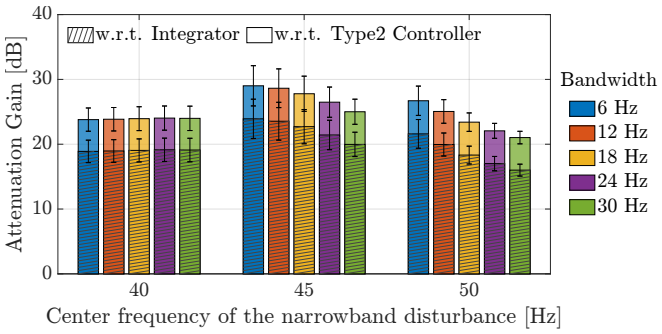

Fig. 7: Attenuation gain of data-driven controller compared to integrator and type2 controller when narrowband disturbance is accounted for during controller design

D. *Effect of external chirp disturbance*

Chirp disturbances, which are transient and naturally damp quickly, might be introduced in the AO system due to some mechanical disruptions. Designing a controller which considers these disturbances might not be useful, but their impact on the performance of the controller needs to be studied. Fig. 8 shows the closed-loop response for different controllers under chirp disturbance. Data-driven controller performs better than the other controllers and is robust to chirp disturbances.

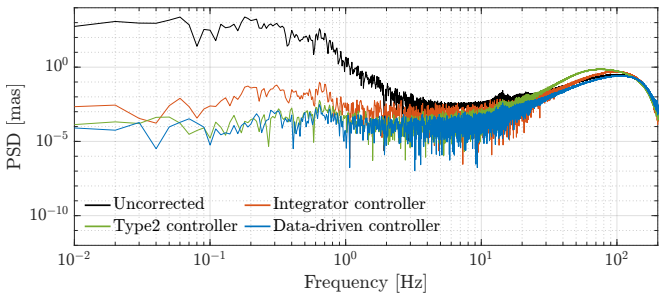

Fig. 8: Closed-loop response under a chirp disturbance

V. Conclusions and Outlook

This paper introduces a robust data-driven vibration control scheme that leverages input-output data from adaptive optics (AO) systems, as well as the disturbance spectrum. The approach offers an intuitive method for defining objectives that accommodate various external disturbances affecting AO systems. The suggested control scheme surpasses existing state-of-the-art controllers and demonstrates enhanced resilience across diverse atmospheric conditions. Moreover, it exhibits notable enhancements for two key categories of external disturbances likely to occur within the telescope's structure: narrowband disturbances originating from electrical components and chirp disturbances stemming from mechanical perturbations. In a subsequent investigation [32], the proposed scheme was implemented and validated on an actual test bench, showcasing improvements of up to 50% in residual error.

References

[1] F. Merkle, P. Kern, P. Léna, F. Rigaut, J. C. Fontanella, G. Rousset, C. Boyer, J. P. Gaffard, and P. Jagourel, "Successful tests of adaptive optics." *The Messenger*, vol. 58, pp. 1–4, Dec. 1989.

[2] W. M. K. Observatory, "Keck pictures of Uranus show best view from the ground," Nov. 2004. [Online]. Available: https://keckobservatory.org/keck_pictures_of_uranus_show_best_view_from_the_ground/

[3] A. Guesalaga, B. Neichel, F. Rigaut, J. Osborn, and D. Guzman, "Comparison of vibration mitigation controllers for adaptive optics systems," *Applied Optics*, vol. 51, no. 19, pp. 4520–4535, Jul. 2012.

[4] B. Ellerbroek and T. Rhoadarmer, "Adaptive wavefront control algorithms for closed loop adaptive optics," *Mathematical and Computer Modelling*, vol. 33, no. 1-3, pp. 145–158, Jan. 2001.

[5] E. Gendron and P. Lena, "Astronomical adaptive optics. I. Modal control optimization," *Astronomy and Astrophysics*, vol. 291, no. 1, pp. 337–347, 1994.

[6] C. Petit, J.-M. Conan, C. Kulcsár, and H.-F. Raynaud, "Linear quadratic Gaussian control for adaptive optics and multiconjugate adaptive optics: Experimental and numerical analysis," *Journal of the Optical Society of America A*, vol. 26, no. 6, p. 1307, 2009.

[7] D. Song, X. Li, and Z. Peng, "Mixed sensitivity H-infinity control of an adaptive optics system," *Optical Engineering*, vol. 55, no. 9, 2016.

[8] C. Dessenne, P.-Y. Madec, and G. Rousset, "Optimization of a predictive controller for closed-loop adaptive optics," *Applied Optics*, vol. 37, no. 21, p. 4623, Jul. 1998.

[9] K. Hinnen, M. Verhaegen, and N. Doelman, "A Data-Driven H_2-Optimal Control Approach for Adaptive Optics," *IEEE Transactions on Control Systems Technology*, vol. 16, no. 3, pp. 381–395, May 2008.

[10] R. Hafeez, F. Archinuk, S. Fabbro, H. Teimoorinia, and J.-P. Véran, "Forecasting wavefront corrections in an adaptive optics system," *Journal of Astronomical Telescopes, Instruments, and Systems*, vol. 8, no. 2, p. 029003, May 2022.

[11] A. P. Wong, B. R. M. Norris, P. G. Tuthill, R. Scalzo, J. Lozi, S. B. Vievard, and O. Guyon, "Predictive control for adaptive optics using neural networks," *Journal of Astronomical Telescopes, Instruments, and Systems*, vol. 7, no. 1, p. 019001, Feb. 2021.

[12] M. A. van Kooten, R. Jensen-Clem, S. Cetre, S. Ragland, C. Bond, J. Fowler, and P. Wizinowich, "Status of predictive wavefront control on Keck II adaptive optics bench: On-sky coronagraphic results," in *Techniques and Instrumentation for Detection of Exoplanets X*, S. B. Shaklan and G. J. Ruane, Eds., vol. 11823. SPIE, Sep. 2021, p. 43.

[13] G. Agapito, B. Giorgio, D. Mari, D. Selvi, A. Tesi, and P. Tesi, "Frequency-based design of Adaptive Optics systems," in *Proceedings of the Third AO4ELT Conference - Adaptive Optics for Extremely Large Telescopes*, Florence, Italy, May 2013.

[14] M. Hast, K. Åström, B. Bernhardsson, and S. Boyd, "PID design by convex-concave optimization," in *2013 European Control Conference (ECC)*, Jul. 2013, pp. 4460–4465.

[15] M. Saeki, "Data-driven loop-shaping design of PID controllers for stable plants," *International Journal of Adaptive Control and Signal Processing*, vol. 28, no. 12, pp. 1325–1340, 2014.

[16] A. Karimi and G. Galdos, "Fixed-order H_∞ controller design for nonparametric models by convex optimization," *Automatica*, vol. 46, no. 8, pp. 1388–1394, Aug. 2010.

[17] S. Boyd, M. Hast, and K. J. Åström, "MIMO PID tuning via iterated LMI restriction," *International Journal of Robust and Nonlinear Control*, vol. 26, no. 8, pp. 1718–1731, 2016.

[18] M. Saeki, M. Ogawa, and N. Wada, "Low-order H_∞ controller design on the frequency domain by partial optimization," *International Journal of Robust and Nonlinear Control*, vol. 20, no. 3, pp. 323–333, Feb. 2010.

[19] A. Karimi, A. Nicoletti, and Y. Zhu, "Robust H_∞ controller design using frequency-domain data via convex optimization," *International Journal of Robust and Nonlinear Control*, vol. 28, no. 12, pp. 3766–3783, 2018.

[20] A. Karimi and C. Kammer, "A data-driven approach to robust control of multivariable systems by convex optimization," *Automatica*, vol. 85, pp. 227–233, Nov. 2017.

[21] L. Simard, D. Crampton, B. Ellerbroek, and C. Boyer, "The TMT Instrumentation Program," in *Proceedings of SPIE*, vol. 7735, 2010, p. 773523.

[22] D. Crampton and B. Ellerbroek, "Design and development of TMT," *Proceedings of the International Astronomical Union*, vol. 1, no. S232, pp. 410–419, 2005.

[23] F. Roddier, "The effects of atmospheric turbulence in optical astronomy," *Progress in Optics*, vol. 19, no. C, pp. 281–376, Jan. 1981.

[24] F. Roddier, Ed., *Adaptive Optics in Astronomy*. Cambridge University Press, 1999.

[25] R. Davies and M. Kasper, "Adaptive optics for astronomy," *Annual Review of Astronomy and Astrophysics*, vol. 50, no. 1, pp. 305–351, Sep. 2012.

[26] M. Born and E. Wolf, *Principles of Optics: Electromagnetic Theory of Propagation, Interference and Diffraction of Light*, 7th ed. Cambridge, U.K.: Cambridge Univ. Press, 1999.

[27] R. Pintelon and J. Schoukens, *System Identification: A Frequency Domain Approach*, 2nd ed. John Wiley & Sons, Ltd, 2012.

[28] J.-P. Véran and G. Herriot, "Type II Woofer-Tweeter Control for NFIRAOS on TMT," in *Frontiers in Optics 2009/Laser Science Xxv/Fall 2009 Osa Optics & Photonics Technical Digest*. Optica Publishing Group, 2009, p. JTuC2.

[29] J.-P. Véran, C. Irvin, A. Beauvillier, and G. Herriot, "Implementation of type-II tip-tilt control in NFIRAOS with woofer-tweeter and vibration cancellation," in *Proceedings of SPIE*, vol. 7736. SPIE, Jul. 2010, p. 77364I.

[30] G. Shagal, D. G. MacMynowski, and K. Vogiatzis, "Finite element analysis of TMT vibrations transmitted through Telescope-Enclosure-Soil Interaction," *Modeling, Systems Engineering, and Project Management for Astronomy III*, vol. 7017, Jul. 2008.

[31] J. Fitzsimmons, D. Andersen, J. Atwood, G. Herriot, D. Kerley, S. Roberts, and J. P. Veran, "Integrated modeling of NFIRAOS: Characterizing performance in the presence of vibration," in *AO4ELT 2019 - Proceedings 6th Adaptive Optics for Extremely Large Telescopes*. AO4ELT6, 2019.

[32] I. B. Dinis, "Data-driven control and two stages AO system for SPHERE instrument," Master's thesis, École Polytechnique Fédérale de Lausanne (EPFL), Lausanne, Switzerland, 2022.